Chapter 7
Wavelets and Multiresolution Processing

FIGURE 7.1 A natural image and its local histogram variations.

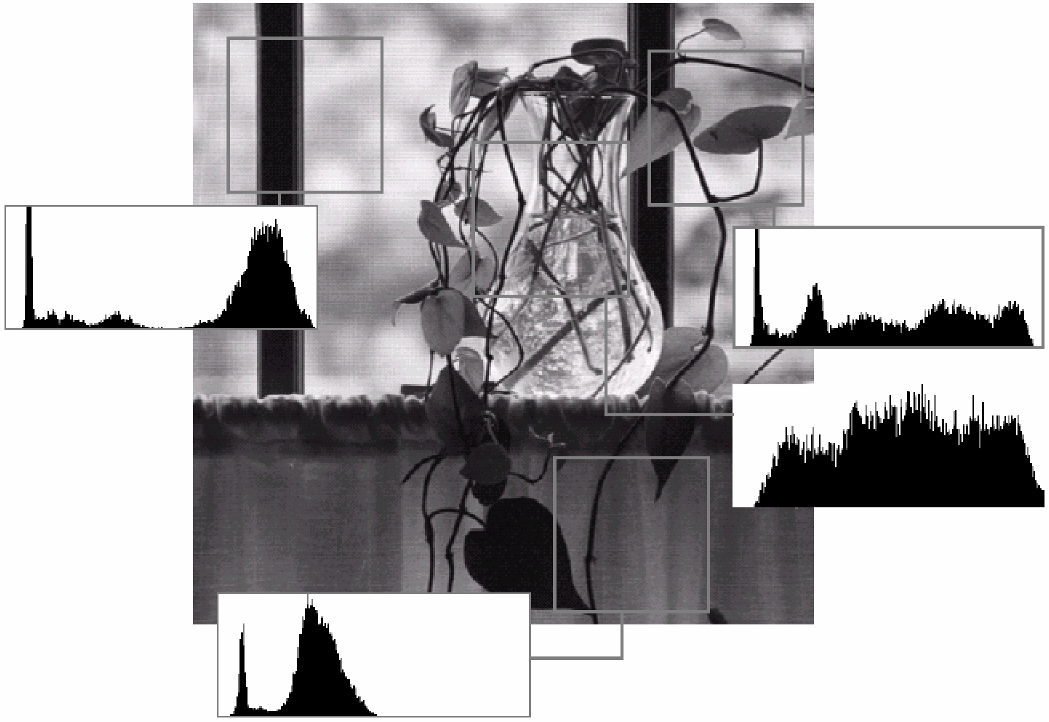

Chapter 7
Wavelets and Multiresolution Processing

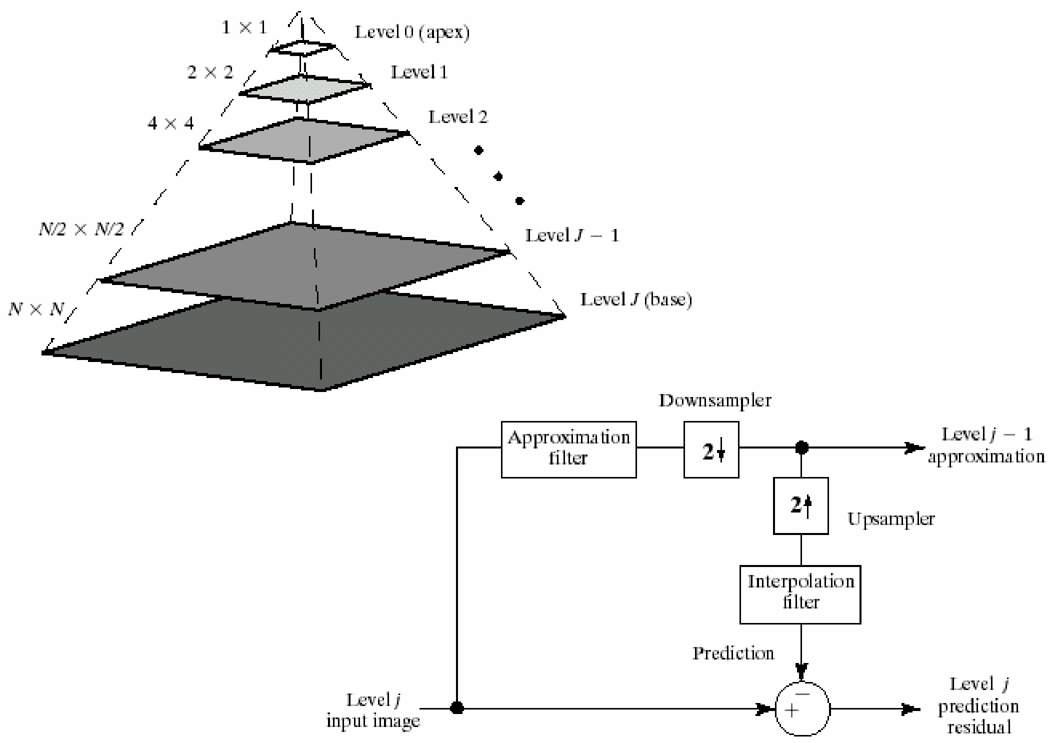

a b

FIGURE 7.2 (a) A pyramidal image structure and (b) system block diagram for creating it.

Chapter 7
Wavelets and Multiresolution Processing

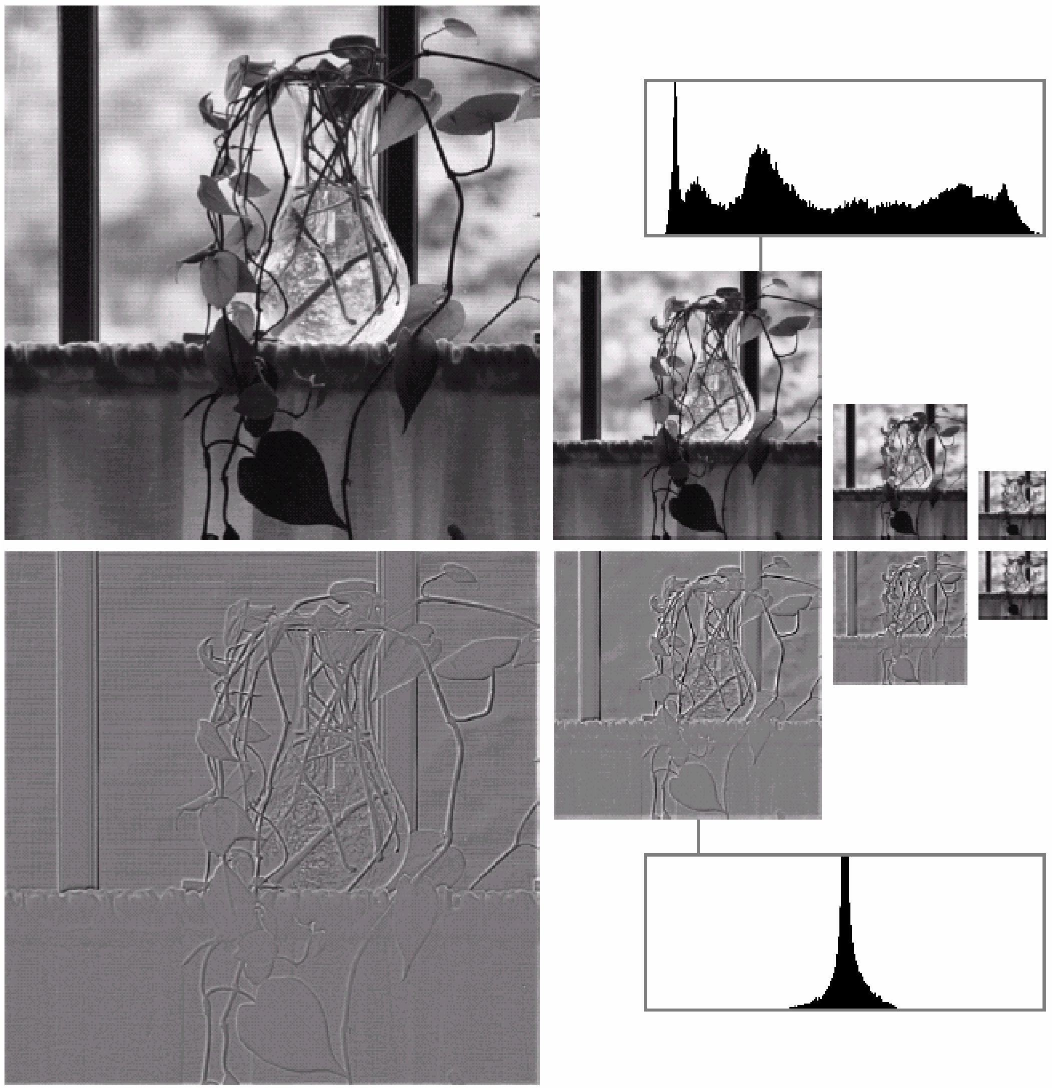

a
b

FIGURE 7.3 Two image pyramids and their statistics: (a) a Gaussian (approximation) pyramid and (b) a Laplacian (prediction residual) pyramid.

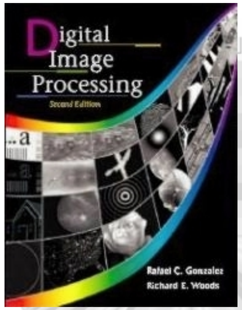

Chapter 7
Wavelets and Multiresolution Processing

a
b

FIGURE 7.4 (a) A two-band filter bank for one-dimensional subband coding and decoding, and (b) its spectrum splitting properties.

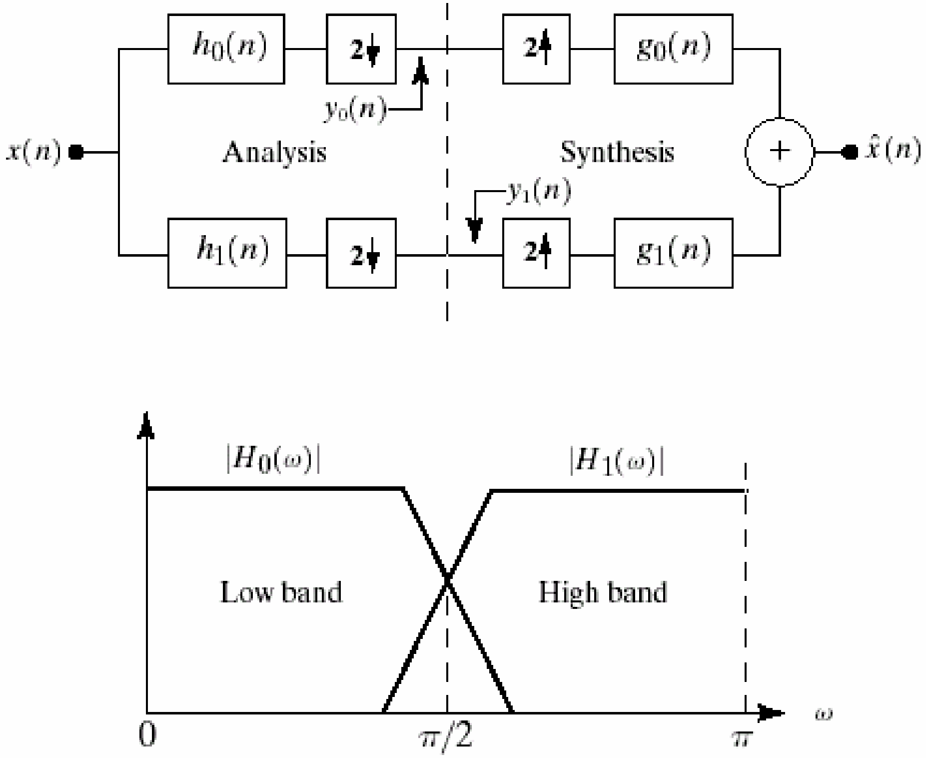

Filter	QMF	CQF	Orthonormal
$H_0(z)$	$H_0^2(z) - H_0^2(-z) = 2$	$H_0(z)H_0(z^{-1}) +$ $H_0^2(-z)H_0(-z^{-1}) = 2$	$G_0(z^{-1})$
$H_1(z)$	$H_0(-z)$	$z^{-1}H_0(-z^{-1})$	$G_1(z^{-1})$
$G_0(z)$	$H_0(z)$	$H_0(z^{-1})$	$G_0(z)G_0(z^{-1}) +$ $G_0(-z)G_0(-z^{-1}) = 2$
$G_1(z)$	$-H_0(-z)$	$zH_0(-z)$	$-z^{-2K+1}G_0(-z^{-1})$

TABLE 7.1 Perfect reconstruction filter families.

Chapter 7
Wavelets and Multiresolution Processing

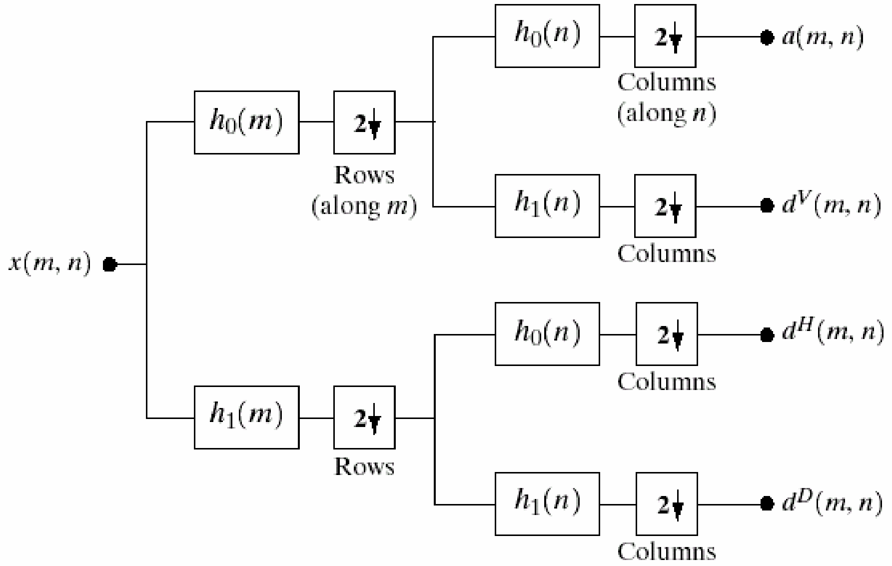

FIGURE 7.5 A two-dimensional, four-band filter bank for subband image coding.

Chapter 7
Wavelets and Multiresolution Processing

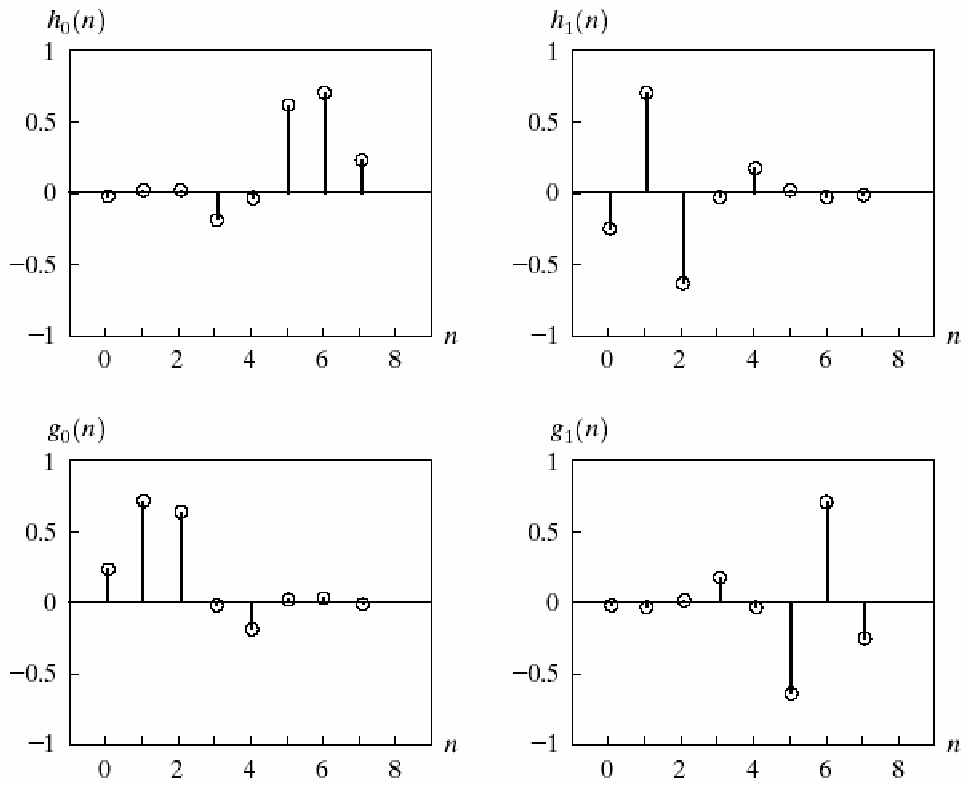

FIGURE 7.6 The impulse responses of four 8-tap Daubechies orthonormal filters.

Chapter 7
Wavelets and Multiresolution Processing

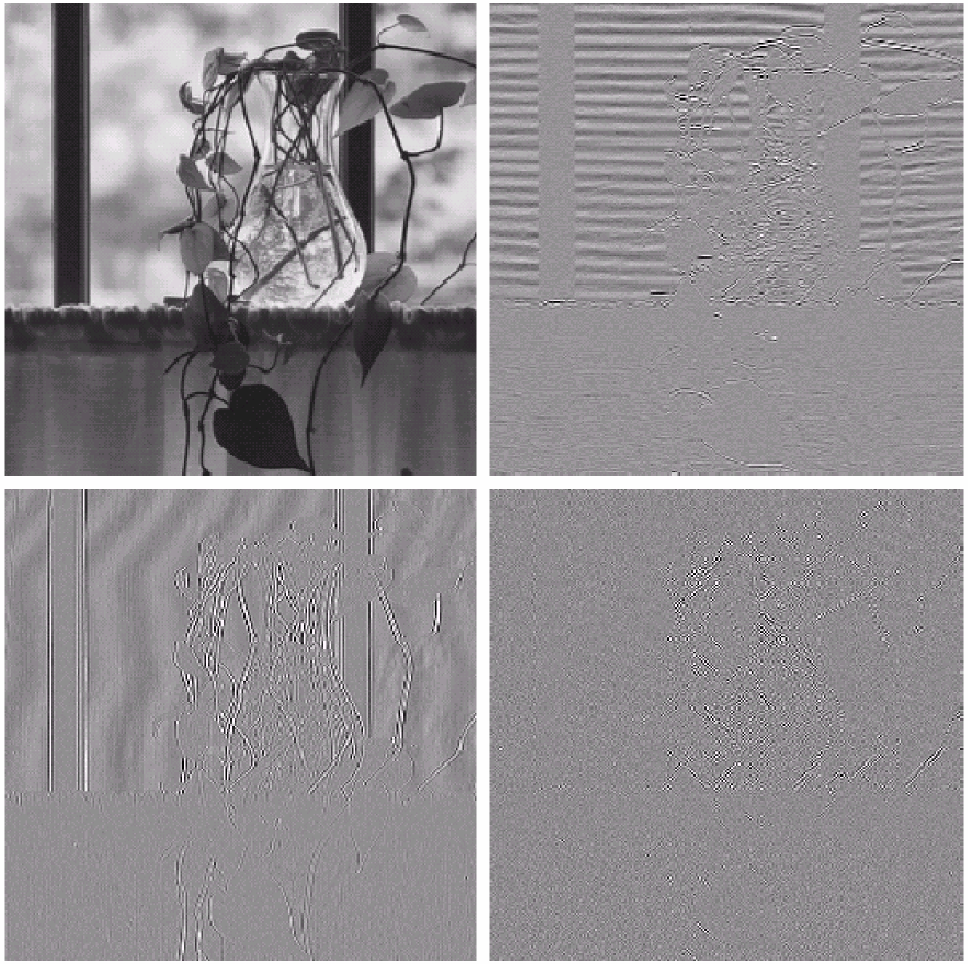

FIGURE 7.7 A four-band split of the vase in Fig. 7.1 using the subband coding system of Fig. 7.5.

Chapter 7
Wavelets and Multiresolution Processing

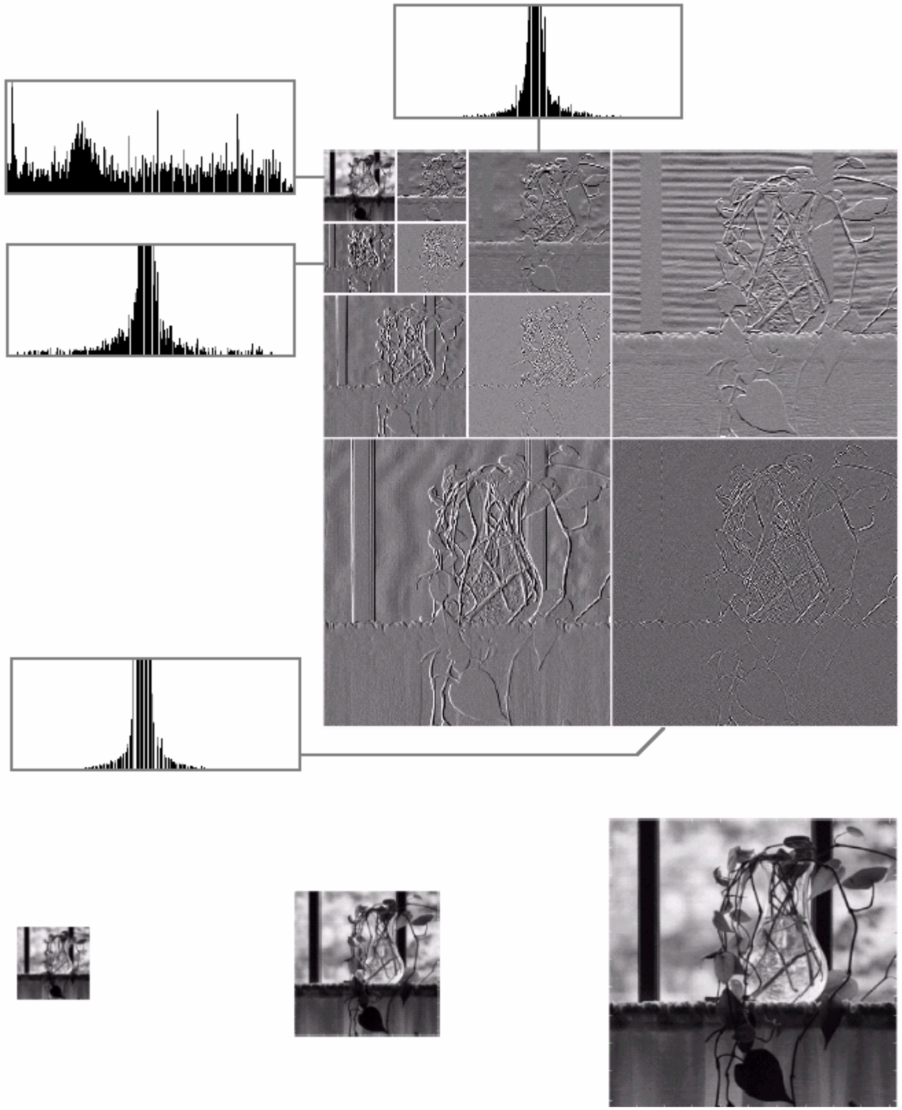

a
b c d

FIGURE 7.8 (a) A discrete wavelet transform using Haar basis functions. Its local histogram variations are also shown; (b)–(d) Several different approximations (64×64, 128×128, and 256×256) that can be obtained from (a).

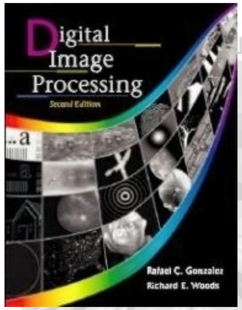

Chapter 7
Wavelets and Multiresolution Processing

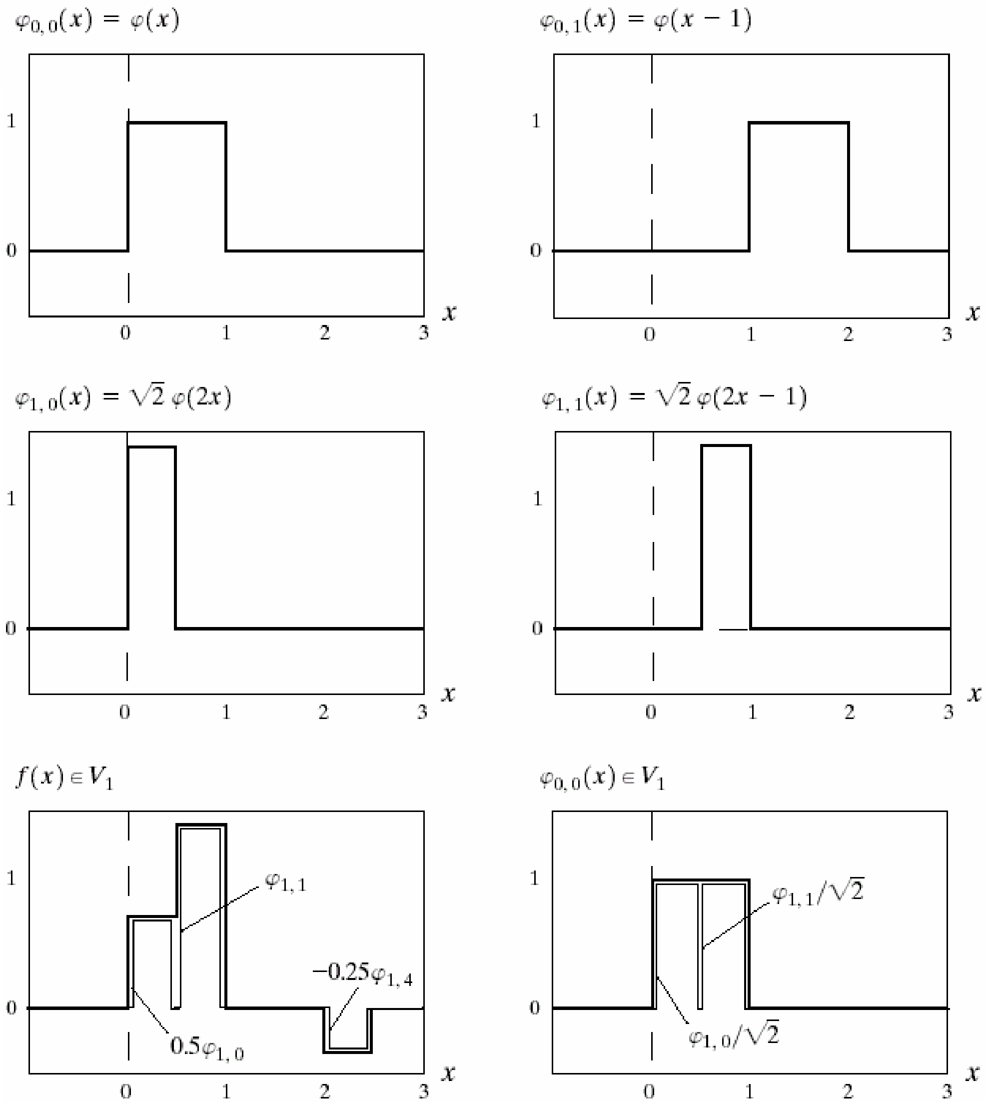

a	b
c	d
e	f

FIGURE 7.9 Haar scaling functions in V_0 in V_1.

Chapter 7
Wavelets and Multiresolution Processing

FIGURE 7.10 The nested function spaces spanned by a scaling function.

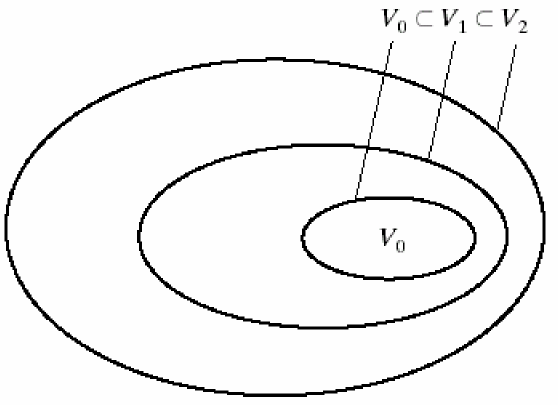

Chapter 7
Wavelets and Multiresolution Processing

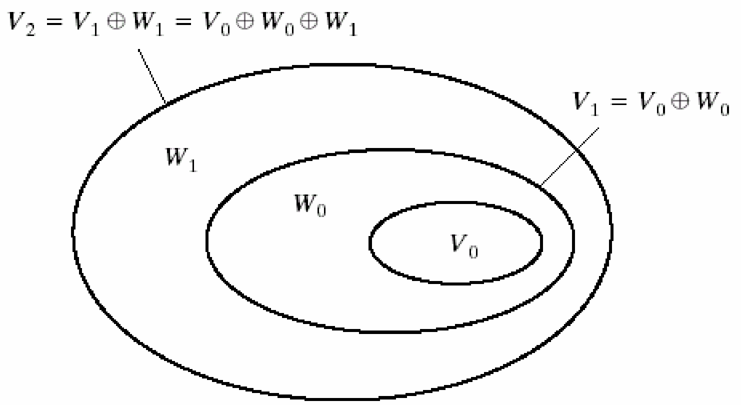

FIGURE 7.11 The relationship between scaling and wavelet function spaces.

Chapter 7
Wavelets and Multiresolution Processing

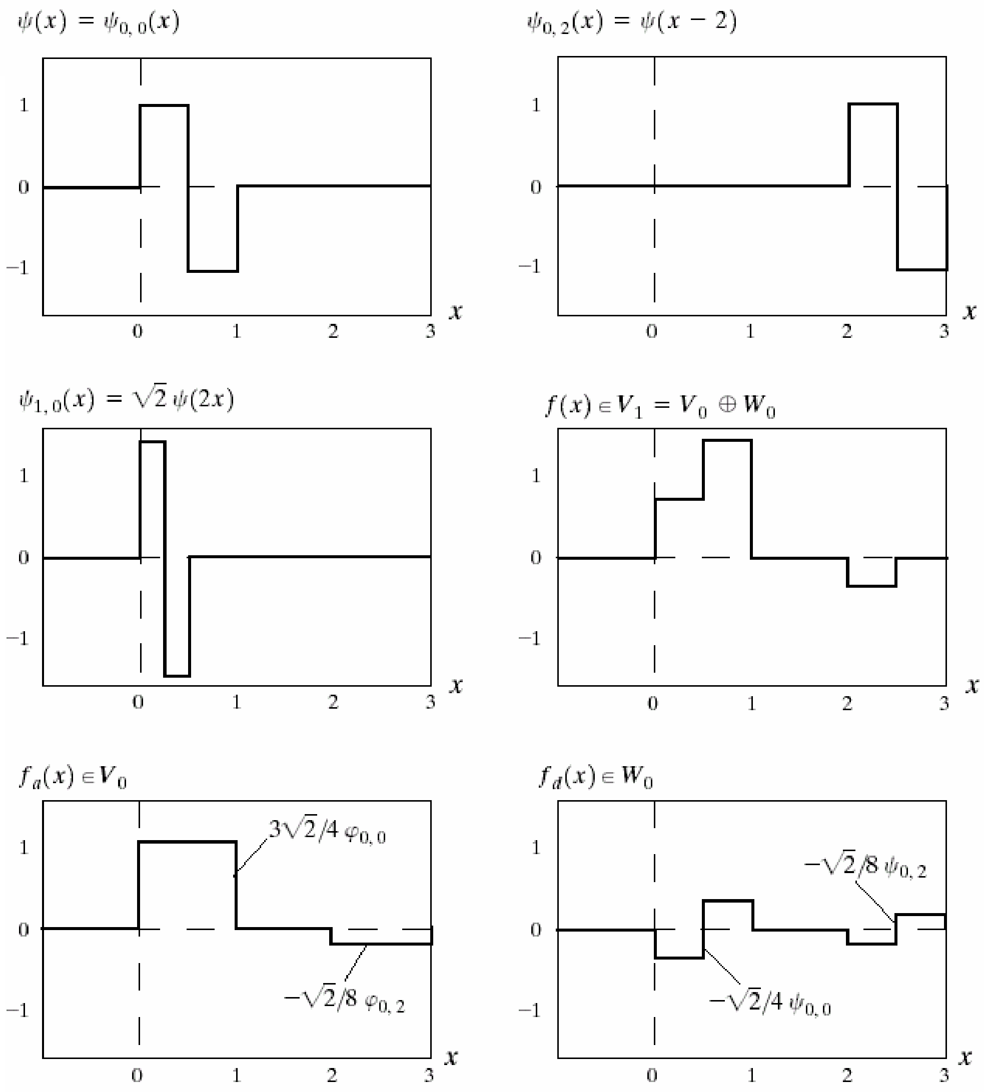

FIGURE 7.12 Haar wavelet functions in W_0 and W_1.

Chapter 7
Wavelets and Multiresolution Processing

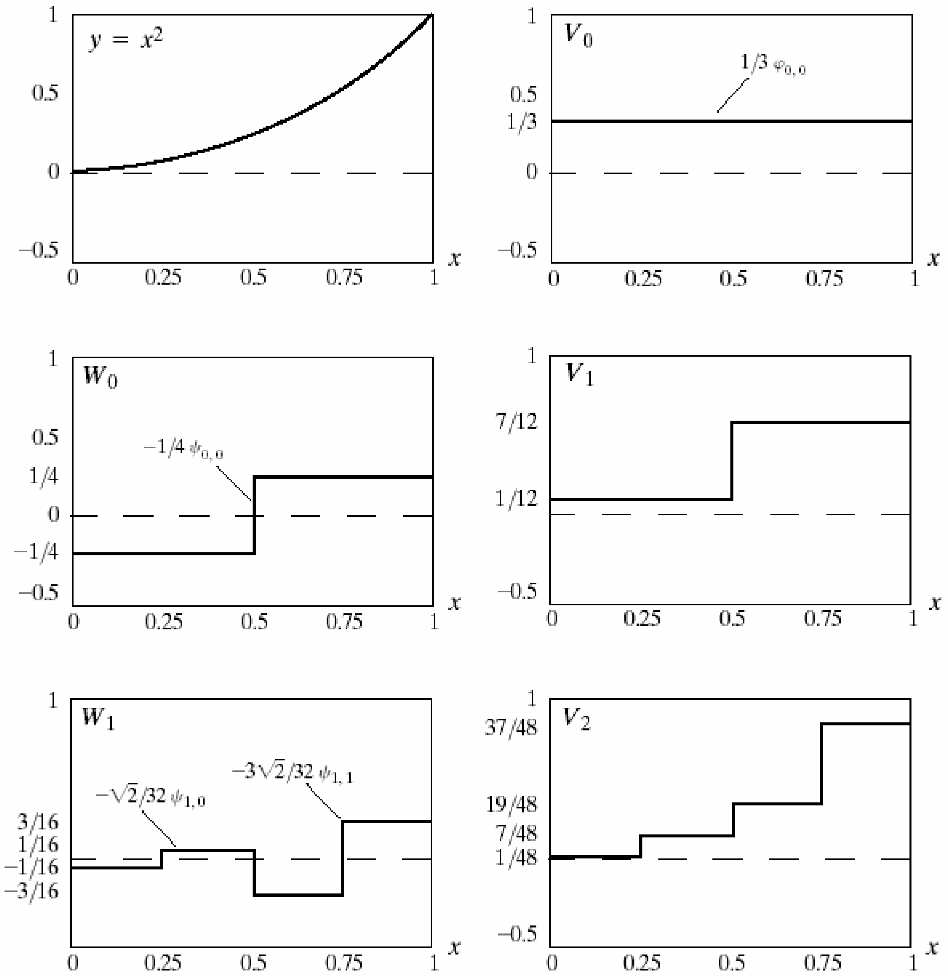

FIGURE 7.13 A wavelet series expansion of $y = x^2$ using Haar wavelets.

Chapter 7
Wavelets and Multiresolution Processing

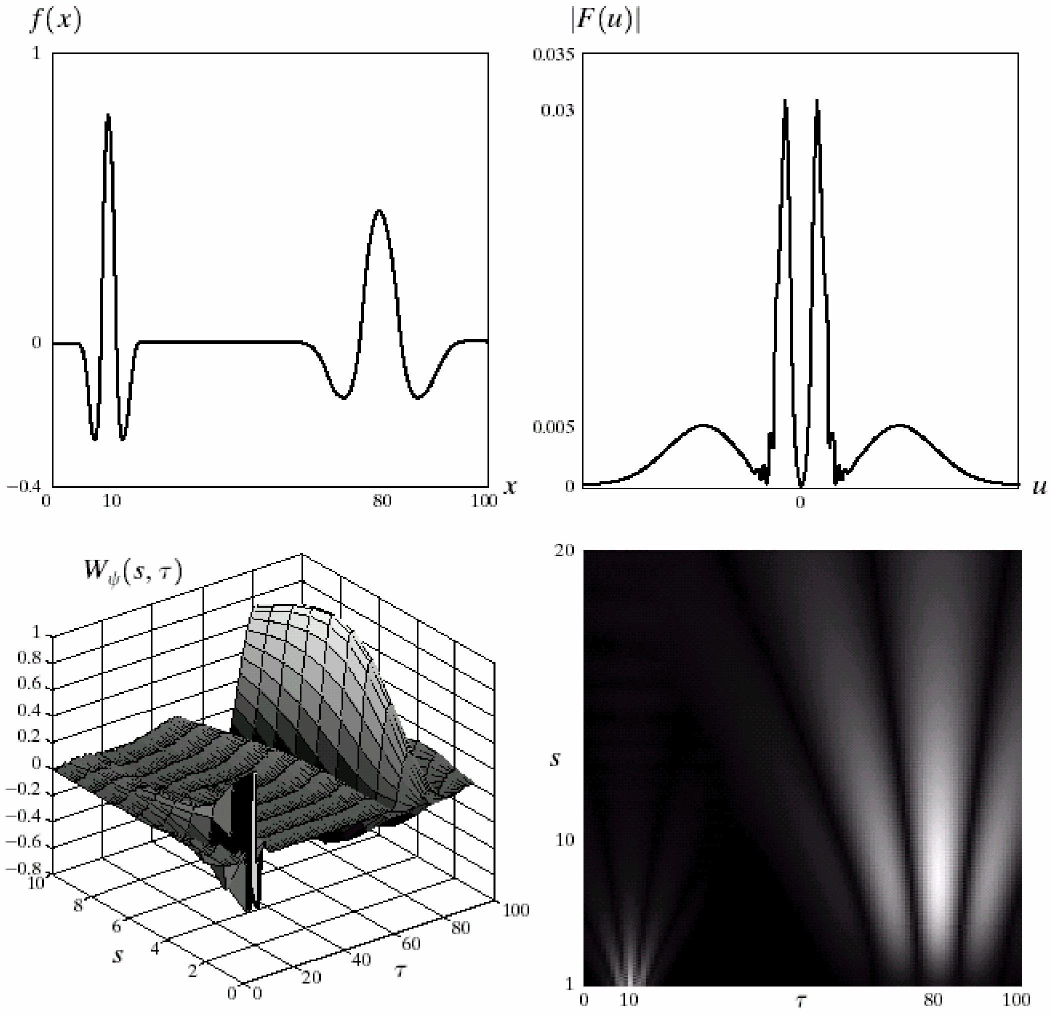

FIGURE 7.14 The continuous wavelet transform (c and d) and Fourier spectrum (b) of a continuous one-dimensional function (a).

Chapter 7
Wavelets and Multiresolution Processing

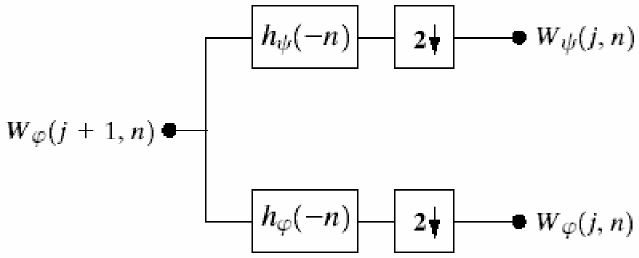

FIGURE 7.15 An FWT analysis bank.

Chapter 7
Wavelets and Multiresolution Processing

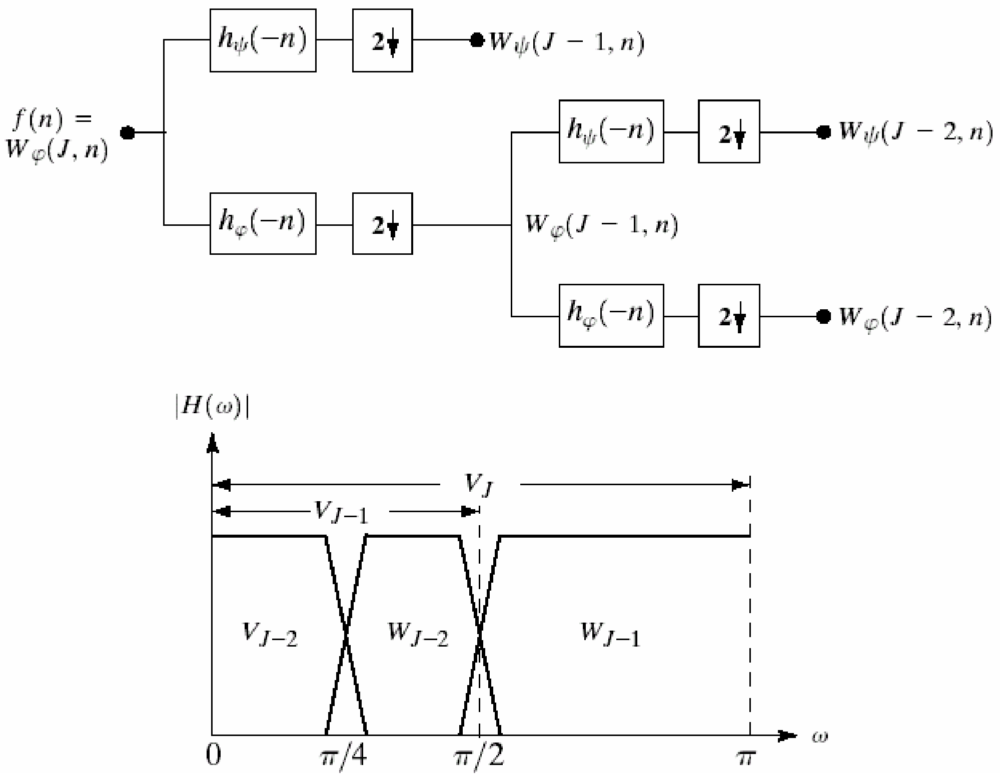

a
b

FIGURE 7.16 (a) A two-stage or two-scale FWT analysis bank and (b) its frequency splitting characteristics.

Chapter 7
Wavelets and Multiresolution Processing

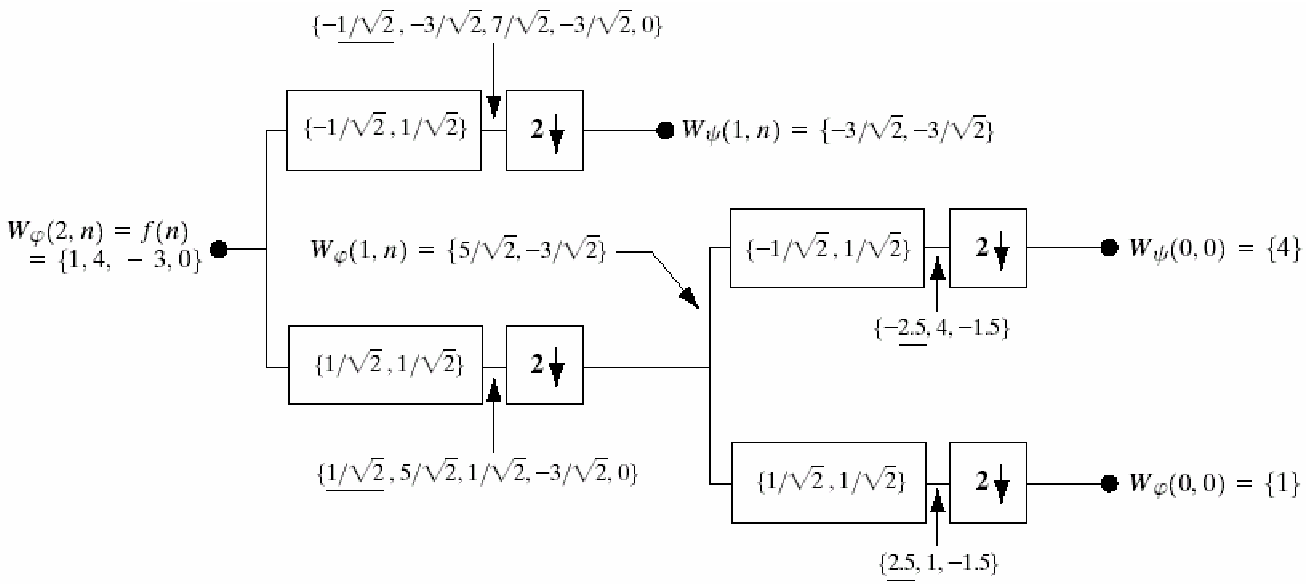

FIGURE 7.17 Computing a two-scale fast wavelet transform of sequence $\{1, 4, -3, 0\}$ using Haar scaling and wavelet vectors.

Chapter 7
Wavelets and Multiresolution Processing

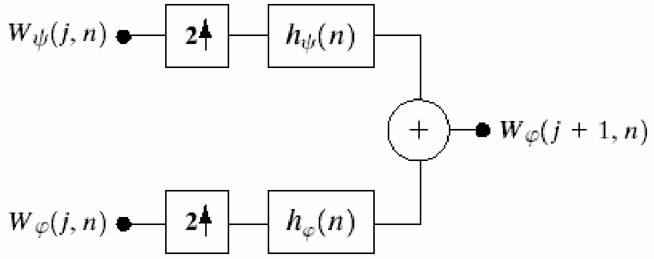

FIGURE 7.18 The FWT^{-1} synthesis filter bank.

Chapter 7
Wavelets and Multiresolution Processing

FIGURE 7.19 A two-stage or two-scale FWT^{-1} synthesis bank.

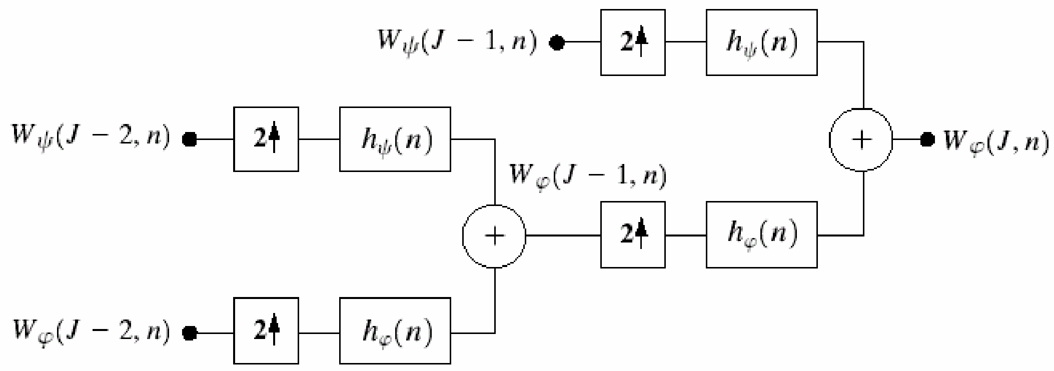

Chapter 7
Wavelets and Multiresolution Processing

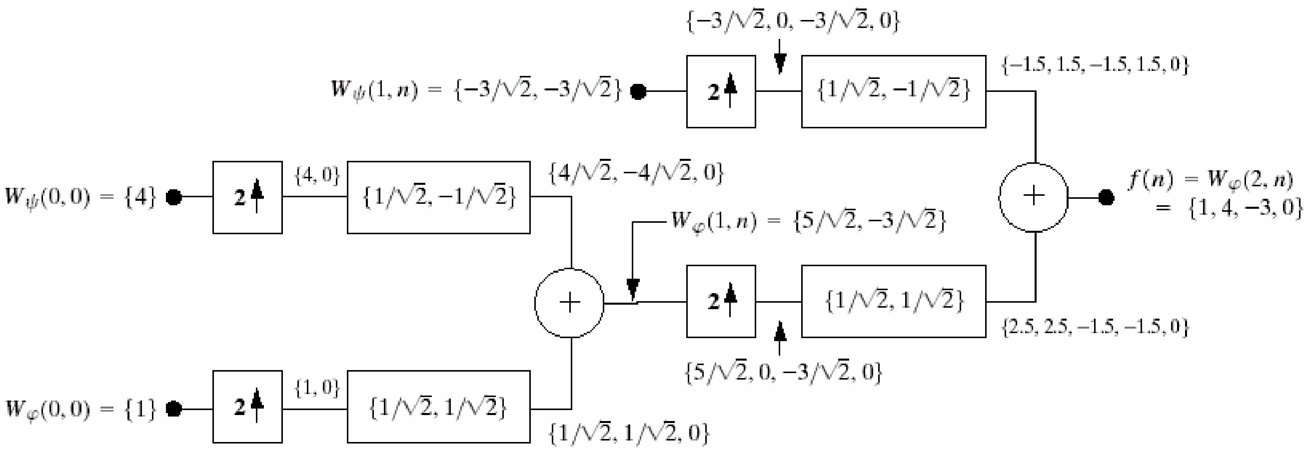

FIGURE 7.20 Computing a two-scale inverse fast wavelet transform of sequence $\{1, 4, -1.5\sqrt{2}, -1.5\sqrt{2}\}$ with Haar scaling and wavelet vectors.

Chapter 7
Wavelets and Multiresolution Processing

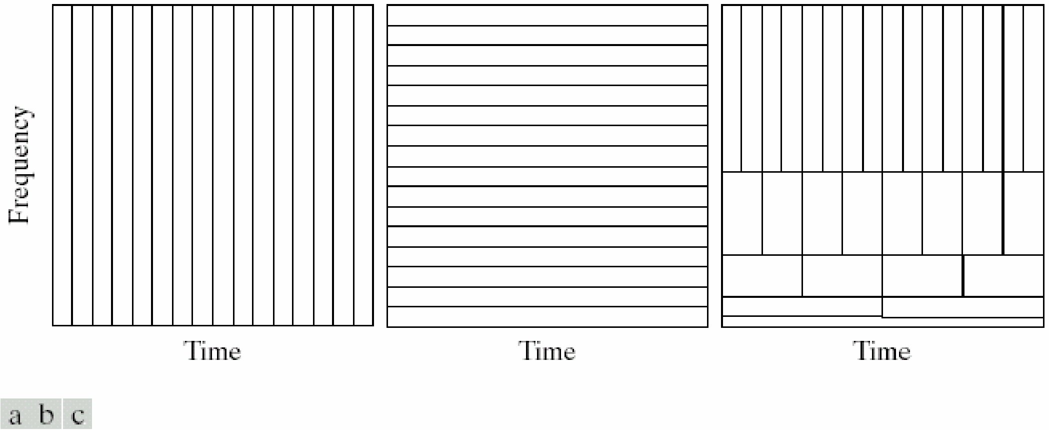

FIGURE 7.21 Time-frequency tilings for (a) sampled data, (b) FFT, and (c) FWT basis functions.

Chapter 7
Wavelets and Multiresolution Processing

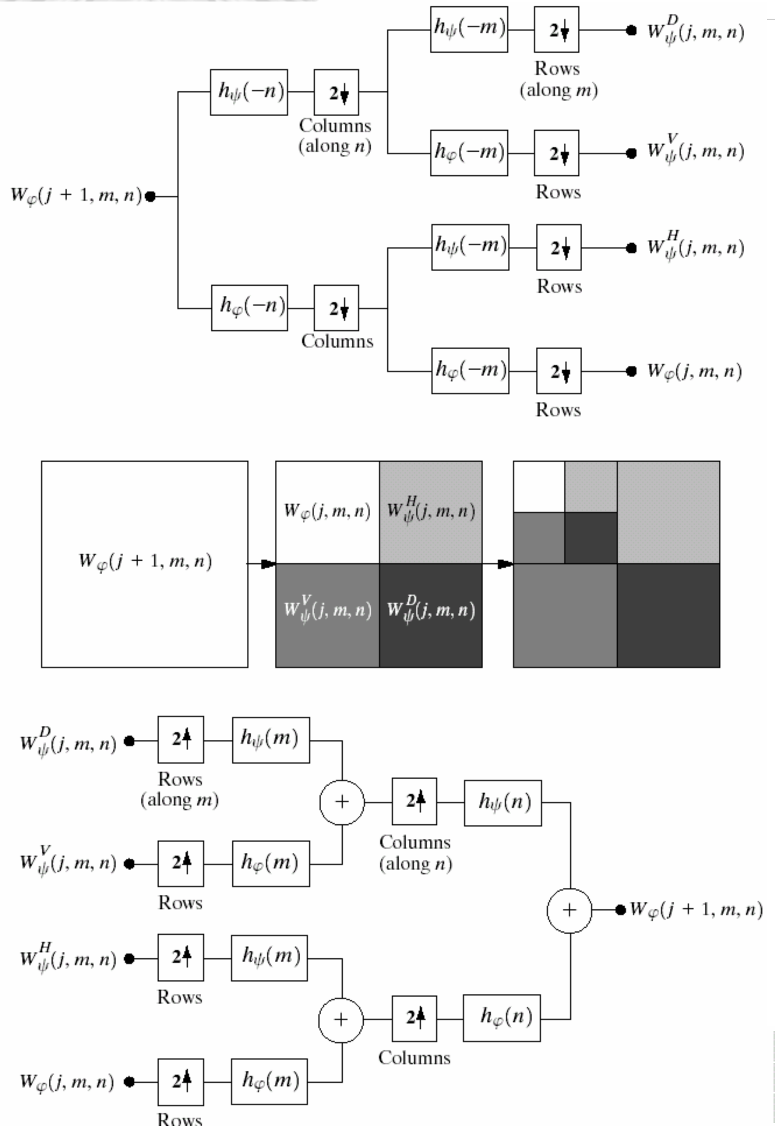

a
b
c

FIGURE 7.22 The two-dimensional fast wavelet transform: (a) the analysis filter bank; (b) the resulting decomposition; and (c) the synthesis filter bank.

Chapter 7
Wavelets and Multiresolution Processing

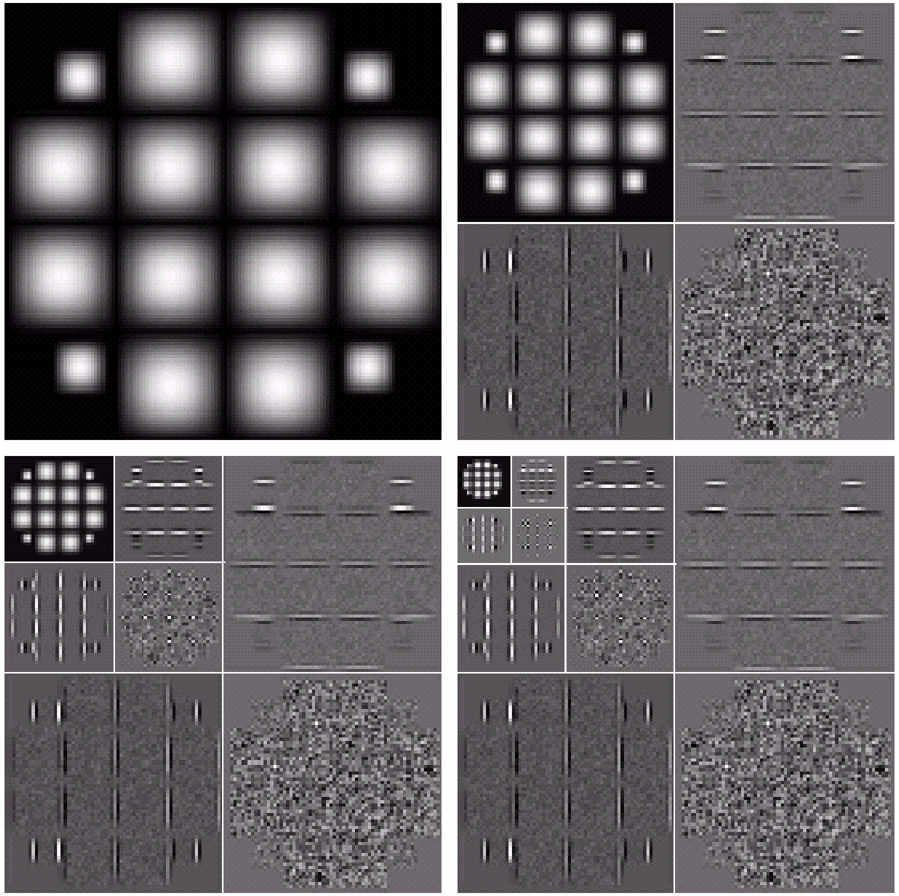

a b
c d

FIGURE 7.23 A three-scale FWT.

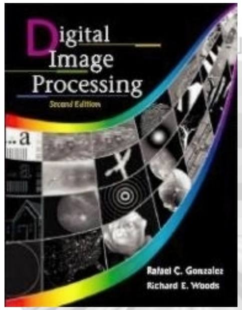

Chapter 7
Wavelets and Multiresolution Processing

a b
c d
e f
g

FIGURE 7.24 Fourth-order symlets: (a)–(b) decomposition filters; (c)–(d) reconstruction filters; (e) the one-dimensional wavelet; (f) the one-dimensional scaling function; and (g) one of three two-dimensional wavelets, $\psi^H(x, y)$.

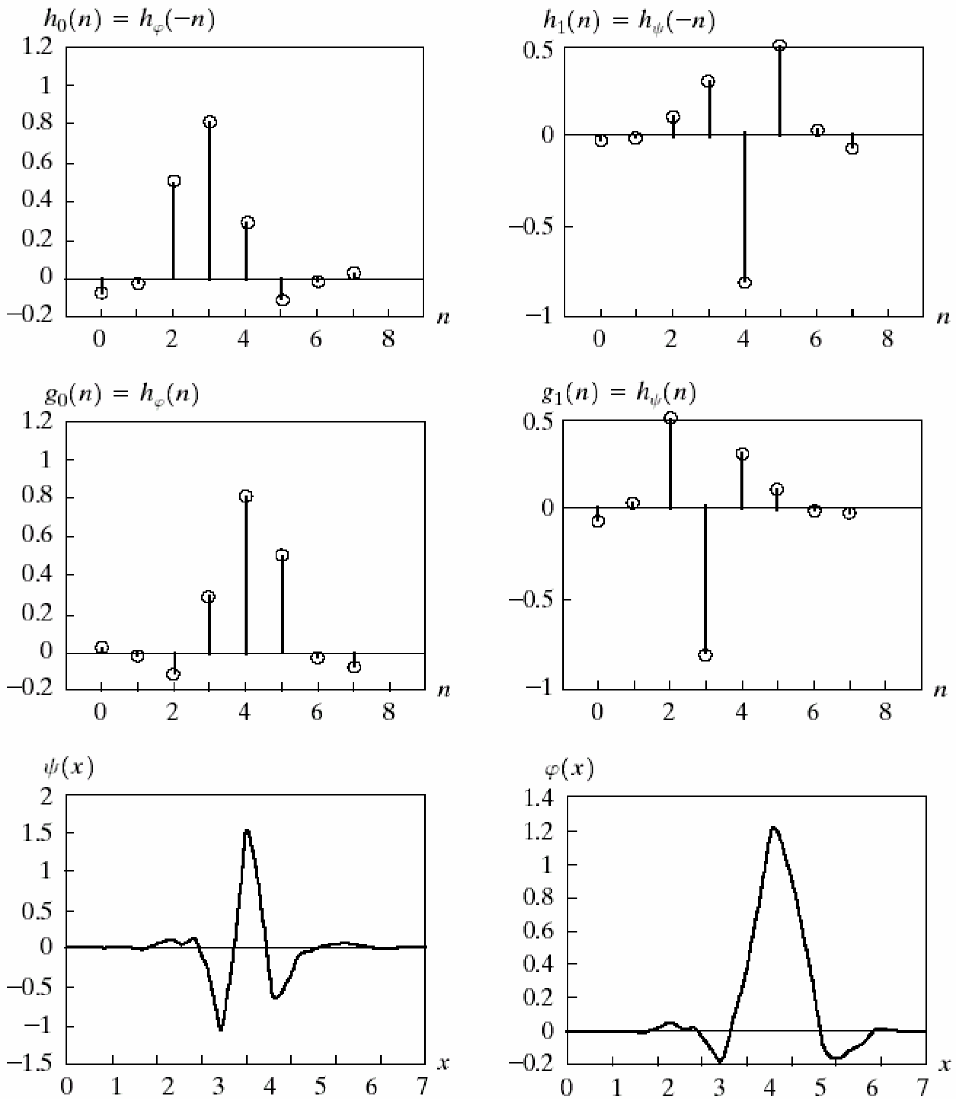

Fig. 7.24 (Con't)

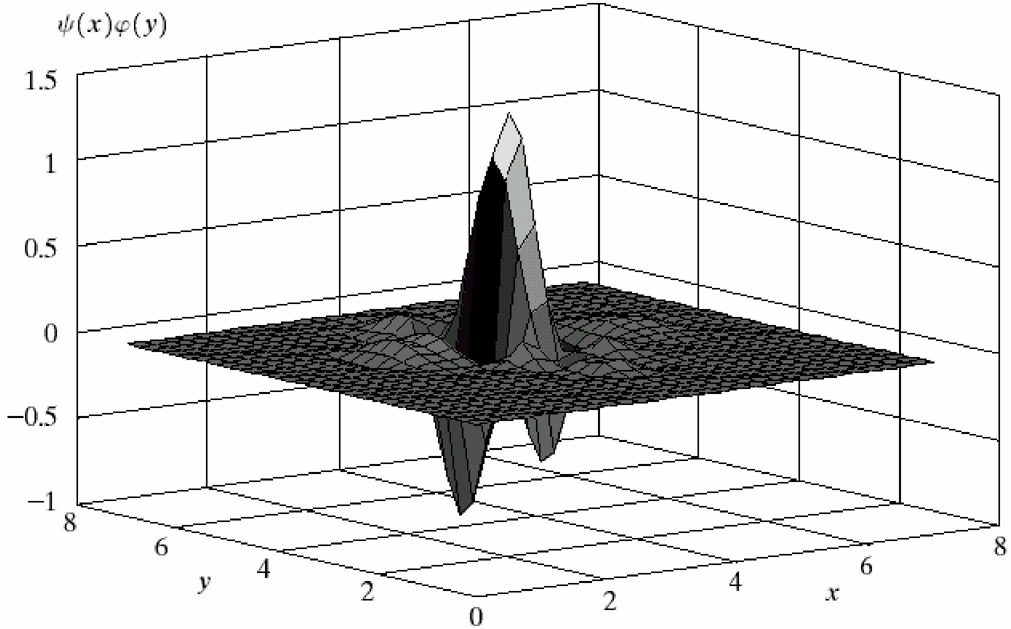

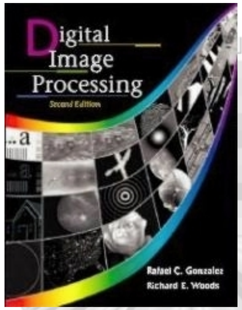

Chapter 7
Wavelets and Multiresolution Processing

a b
c d

FIGURE 7.25 Modifying a DWT for edge detection: (a) and (c) two-scale decompositions with selected coefficients deleted; (b) and (d) the corresponding reconstructions.

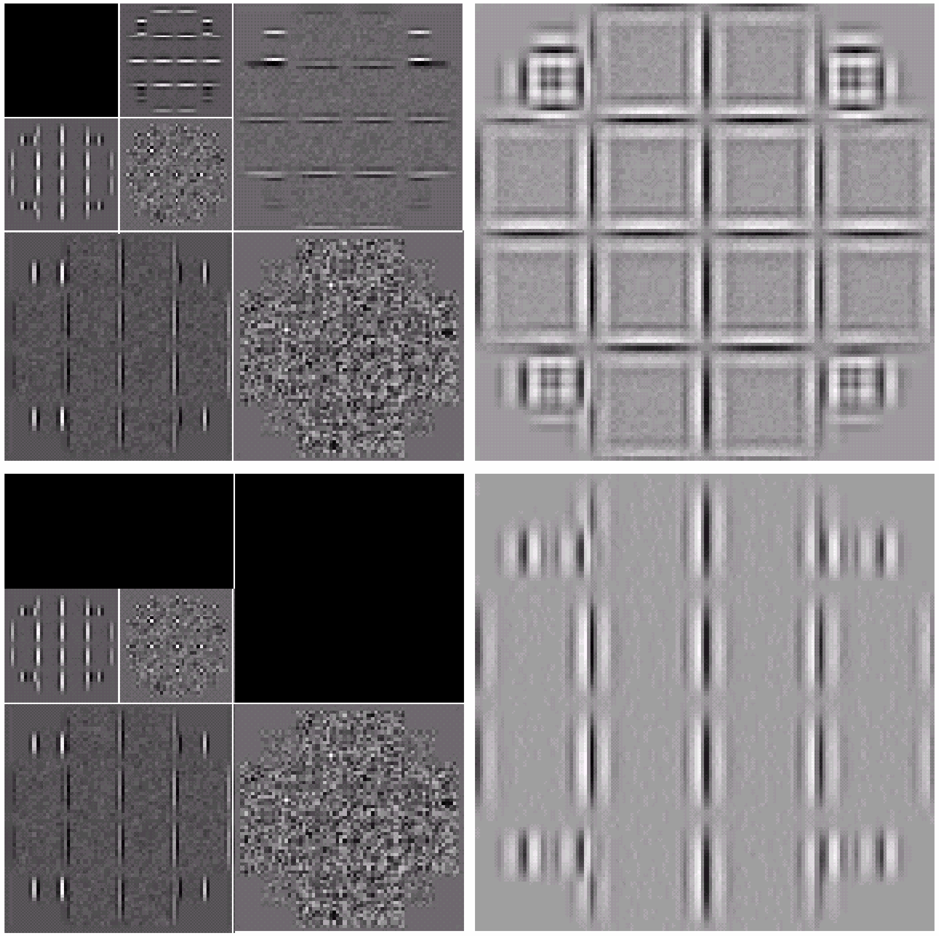

Chapter 7
Wavelets and Multiresolution Processing

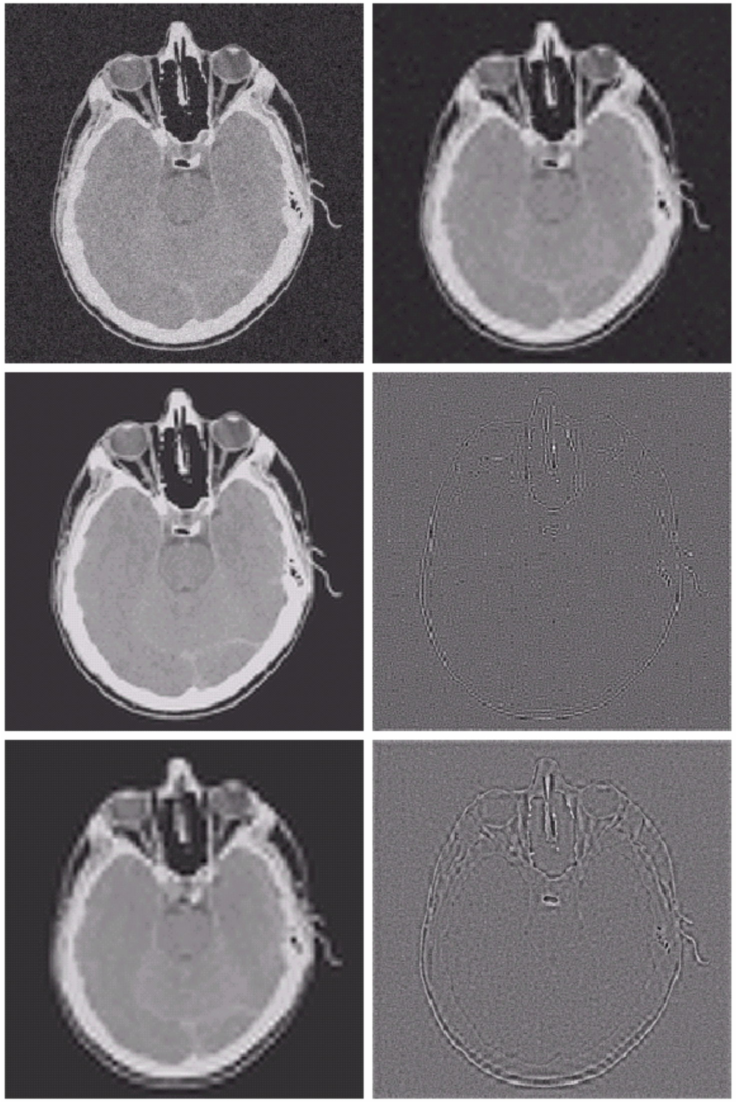

a	b
c	d
e	f

FIGURE 7.26 Modifying a DWT for noise removal: (a) a noisy MRI of a human head; (b), (c) and (e) various reconstructions after thresholding the detail coefficients; (d) and (f) the information removed during the reconstruction of (c) and (e). (Original image courtesy Vanderbuilt University Medical Center.)

Chapter 7
Wavelets and Multiresolution Processing

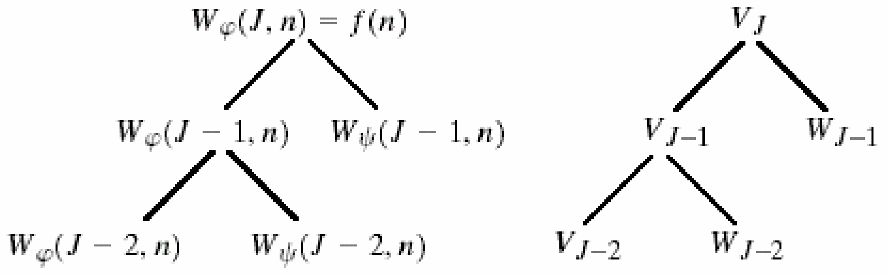

a b

FIGURE 7.27 A coefficient (a) and analysis (b) tree for the two-scale FWT analysis bank of Fig. 7.16.

Chapter 7
Wavelets and Multiresolution Processing

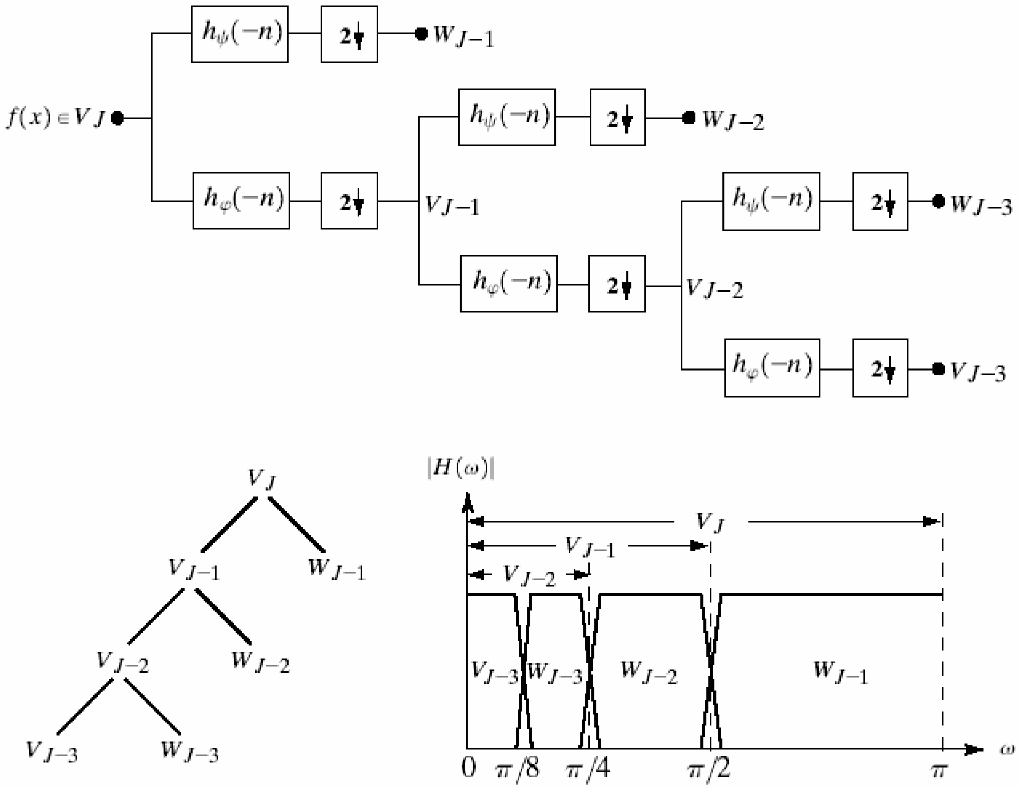

a
b c

FIGURE 7.28 A three-scale FWT filter bank: (a) block diagram; (b) decomposition space tree; and (c) spectrum splitting characteristics.

Chapter 7
Wavelets and Multiresolution Processing

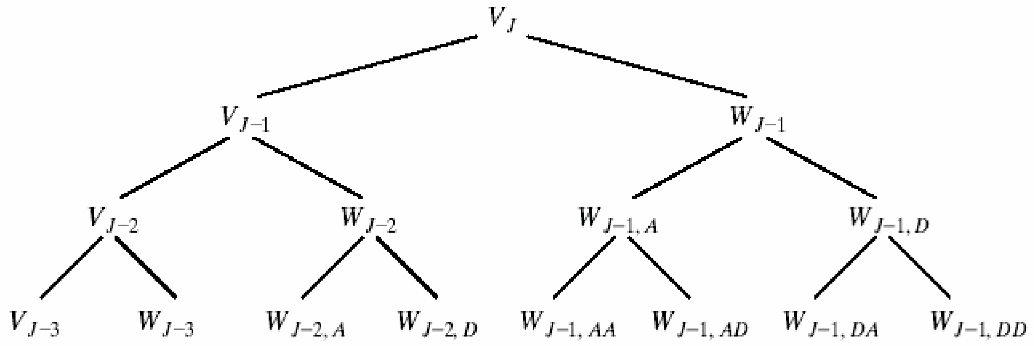

FIGURE 7.29 A three-scale wavelet packet analysis tree.

Chapter 7
Wavelets and Multiresolution Processing

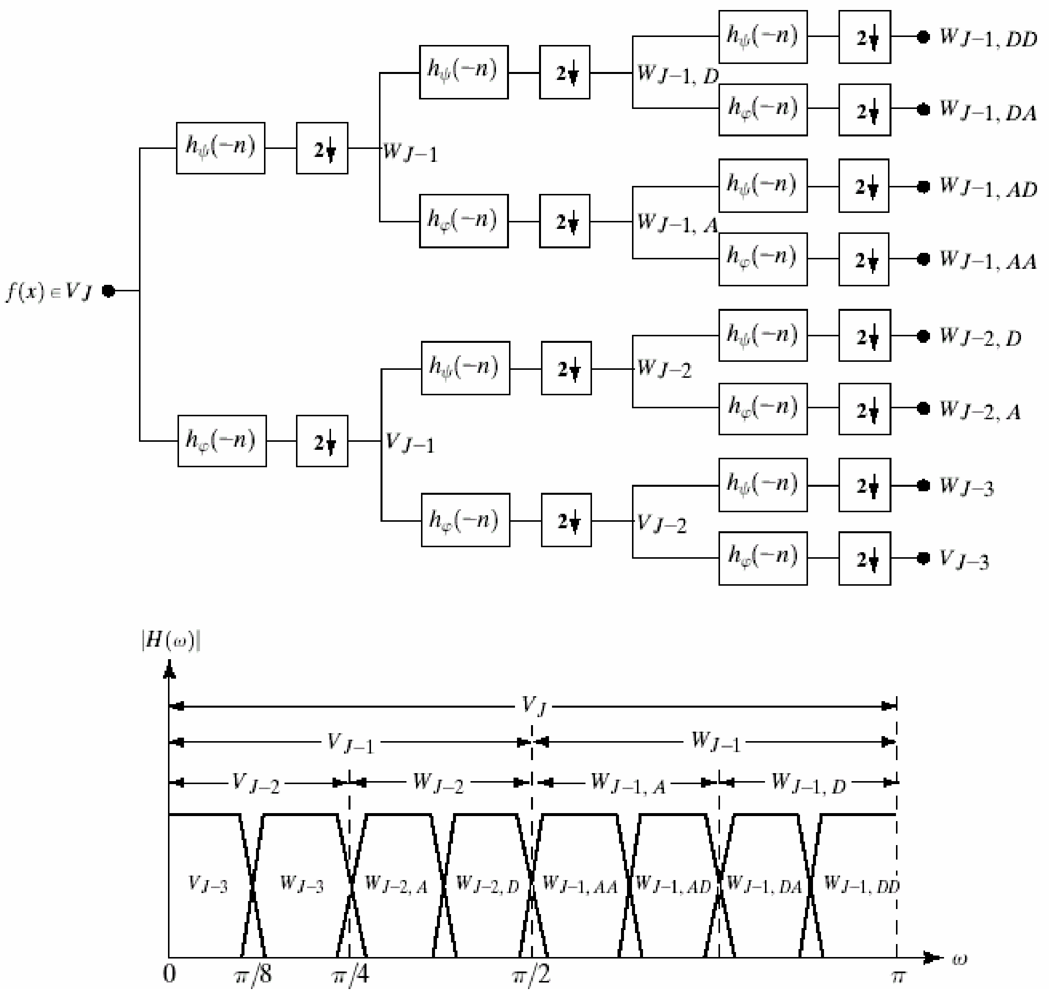

a
b

FIGURE 7.30 The (a) filter bank and (b) spectrum splitting characteristics of a three-scale full wavelet packet analysis tree.

Chapter 7
Wavelets and Multiresolution Processing

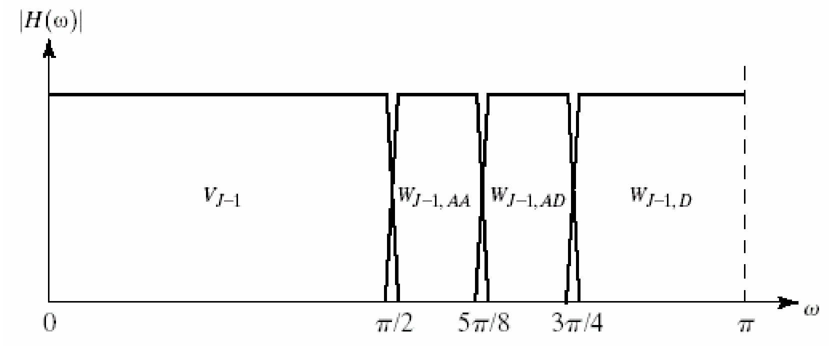

FIGURE 7.31 The spectrum of the decomposition in Eq. (7.6-5).

Chapter 7
Wavelets and Multiresolution Processing

a b

FIGURE 7.32 The first decomposition of a two-dimensional FWT: (a) the spectrum and (b) the subspace analysis tree.

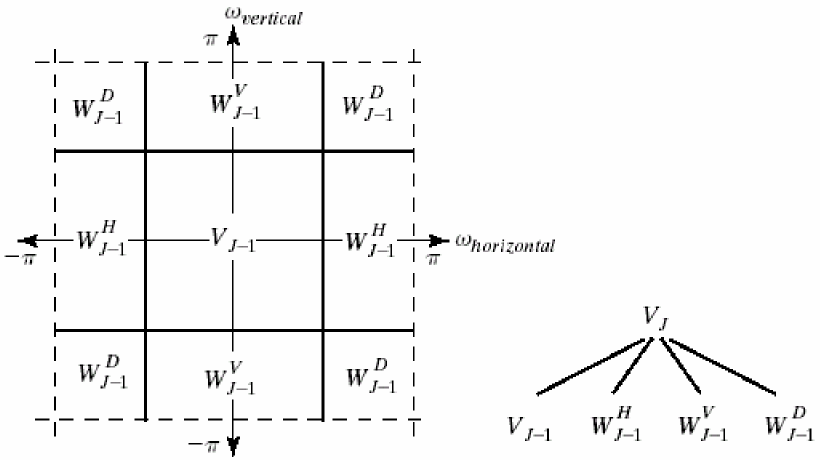

Chapter 7
Wavelets and Multiresolution Processing

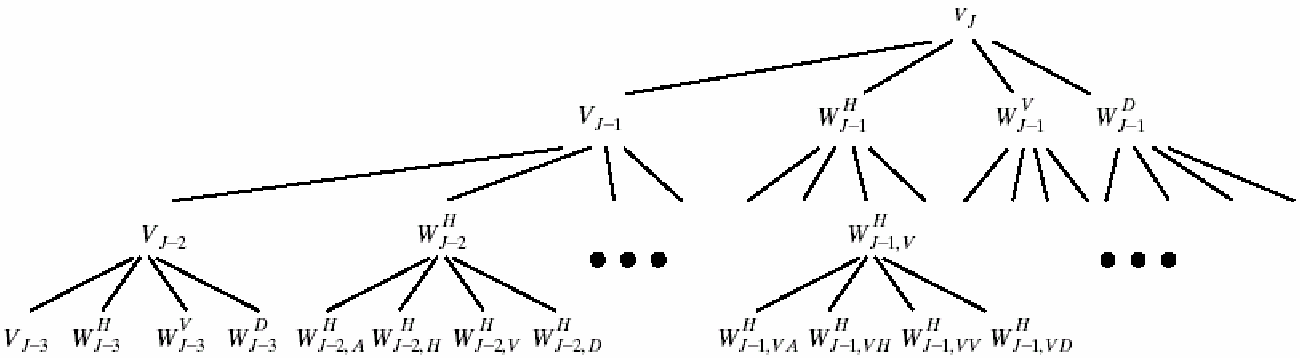

FIGURE 7.33 A three-scale, full wavelet packet decomposition tree. Only a portion of the tree is provided.

Chapter 7
Wavelets and Multiresolution Processing

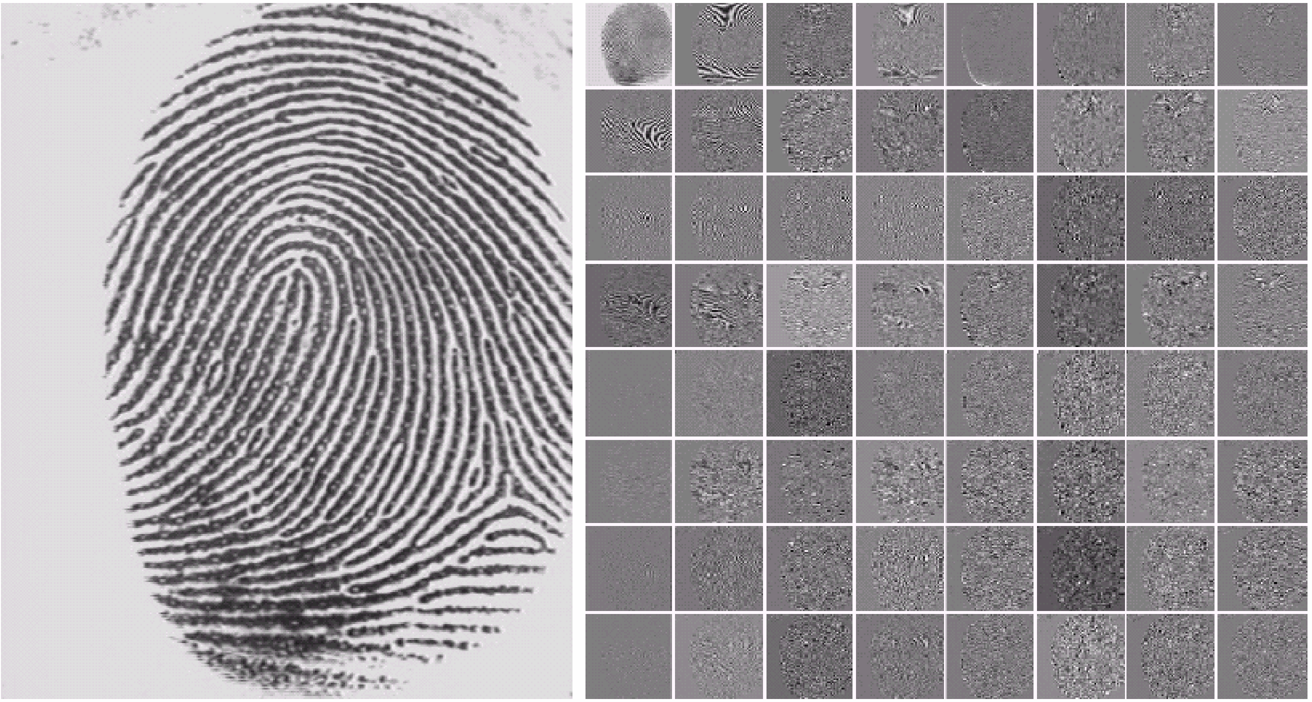

a b

FIGURE 7.34 (a) A scanned fingerprint and (b) its three-scale, full wavelet packet decomposition. (Original image courtesy of the National Institute of Standards and Technology.)

Chapter 7
Wavelets and Multiresolution Processing

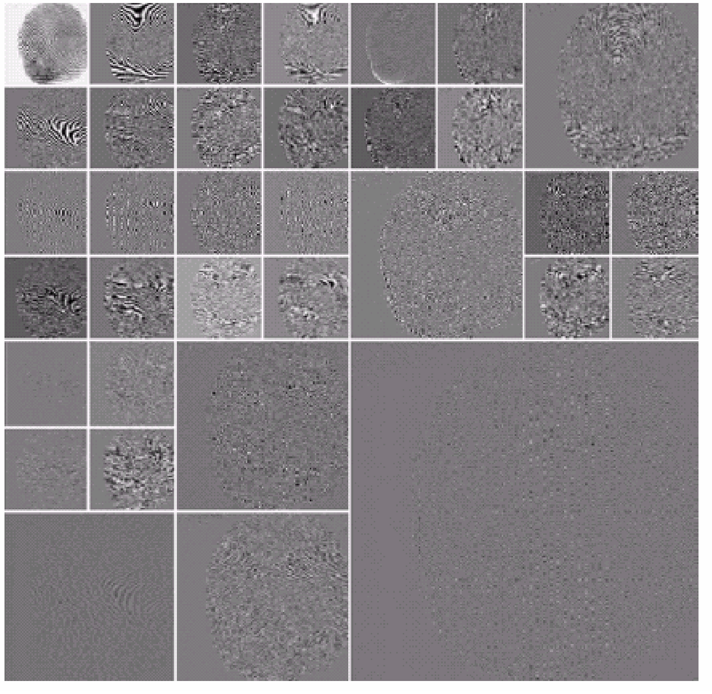

FIGURE 7.35 An optimal wavelet packet decomposition for the fingerprint of Fig. 7.34(a).

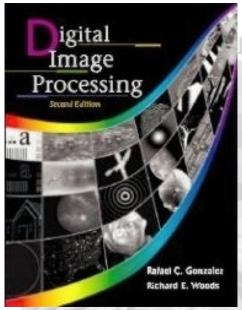

Chapter 7
Wavelets and Multiresolution Processing

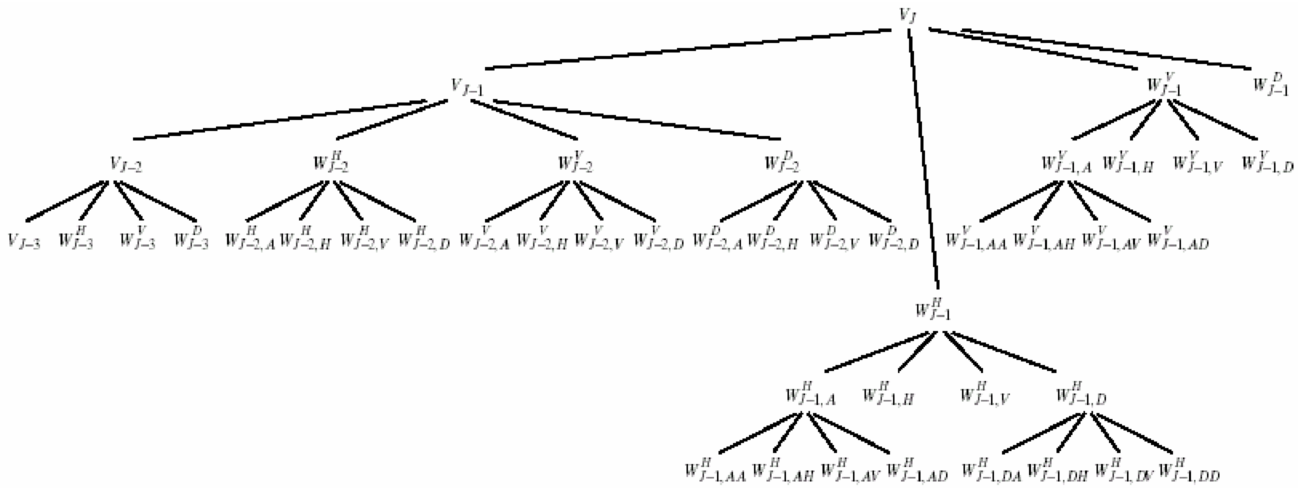

FIGURE 7.36 The optimal wavelet packet analysis tree for the decomposition in Fig. 7.35.

Chapter 7
Wavelets and Multiresolution Processing

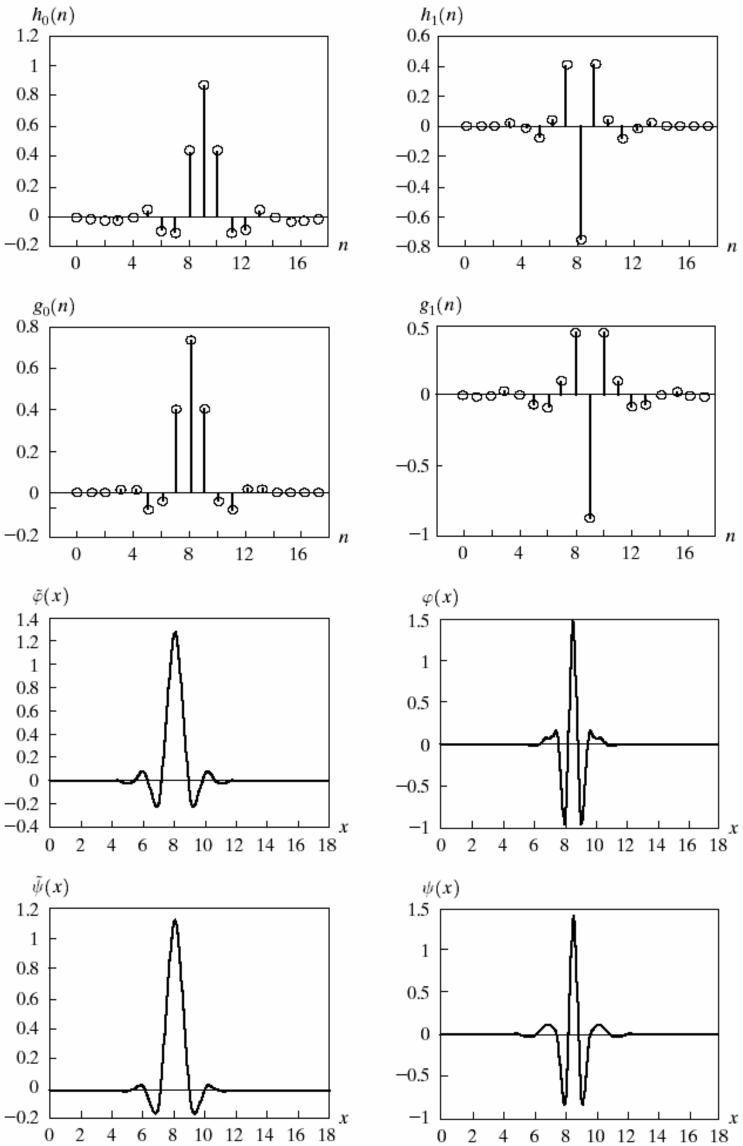

a b
c d
e f
g h

FIGURE 7.37 A member of the Cohen-Daubechies-Feauveau biorthogonal wavelet family: (a) and (b) decomposition filter coefficients; (c) and (d) reconstruction filter coefficients; (e)–(h) dual wavelet and scaling functions.